COUPLED SHELL–FLUID INTERACTION PROBLEMS WITH DEGENERATE SHELL AND THREE-DIMENSIONAL FLUID ELEMENTS

R. K. Singh,† T. Kant‡ and A. Kakodkar†

†Reactor Engineering Division, Bhabha Atomic Research Centre, Trombay, Bombay 400 085, India
‡Department of Civil Engineering, Indian Institute of Technology, Powai, Bombay 400 076, India

Abstract—Discrete methods for practical coupled three-dimensional fluid-structure interaction problems are developed. A C^0 explicitly integrated two-dimensional degenerate shell element and a three-dimensional fluid element are coupled to study shell dynamics, fluid transient and coupled shell–fluid interaction problems. The method of partitioning is used to integrate the fluid and shell meshes in a staggered fashion in an optimum manner. Effective explicit–implicit partitioning is shown to achieve high computational efficiency for this type of problem.

1. INTRODUCTION

Fluid–structure interaction problems have attracted a great deal of attention from the nuclear, space and offshore industries. The important areas of applications are the analysis of liquid containers subjected to earthquake ground motion, resulting in impulsive and sloshing motion of the contained liquid, analysis of submerged structures and components subjected to pressure pulses generated due to accidents or otherwise, and analysis of fluid reservoirs supposed to contain accident-induced high-pressure fluid. Most of the attempts for the transient analysis of such problems have been limited to simplified two-dimensional studies. The three-dimensional transient analysis poses problems in terms of size of the problem and large storage and CPU time required by the computer. The analysis is prone to further difficulties in terms of storage space/CPU time if the structure shows nonlinear behaviour and/or if the fluid undergoes large motions or if the fluid behaviour is governed by some additional field variables such as temperature, phase, etc. Fluid–structure interaction studies are characterized by the oscillations induced in fluid and its effect on the surrounding structures. Moreover, the structure displacements also alter the fluid response. Thus this phenomenon has to be studied in a coupled manner. Some simplified approaches are also available in which the fluid–structure interaction problem is studied in a decoupled manner. The fluid response is first obtained assuming the structure to be rigid and the resulting pressure field is imposed on the structure to obtain the structural response. This approach overestimates the structural response in many cases. Moreover, if coupled modes are excited, this approach gives unconservative results [1–4]. Another simplified method of design has been to use the added mass approach,

treating the fluid as incompressible. This approach will be suitable for a case when fluid oscillation frequencies are sufficiently separated from a structure's predominant frequencies. Thus there is a need to study the fluid–structure interaction problems in a coupled manner.

Earlier studies on fluid–structure interaction problems were made by Bathe and Hahn [1], Liu [4], Akkas *et al.* [5], Wilson and Khalvati [6], Shantaram *et al.* [7] and Deshpande *et al.* [8]. The basic methodology in these studies was to modify an existing structure dynamics code to account for the effect of fluid motion. In this method the shear modulus is set to zero in the fluid domain. The fluid–structure interface is constrained to have normal displacement continuity. The eigenvalue analysis indicates the presence of zero energy modes as described by Akkas *et al.* [5]. Wilson and Khalvati [6] have suggested a method to select an optimum penalty parameter so that these spurious modes can be suppressed. In this approach an irrotational flow condition is enforced. Deshpande *et al.* [8] have also come up with an optimum penalty parameter to couple the structure and fluid meshes which is a function of the density of fluid and the acoustic speed in the fluid medium. Au-Yang and Galford [9] define this method as structure mechanics priority or continuum mechanics approach. This approach is advantageous only for a limited class of problems, such as the linear behaviour of a fluid. Moreover, it does not prove to be economical for a three-dimensional transient analysis, even in the case of a linear problem, due to the large size of the fluid domain; the number of discrete equations becomes very large.

Another approach with which to tackle such a coupled problem is to couple a structure dynamics code with a fluid transient code as described in [9–14]. Historically, this second approach is older than the

first approach. However it has not gained popularity until recently. The major limitation of this method is that the resulting coupled equations from the two fields make the system of equations unsymmetric. The bandwidth becomes very large due to fluid–structure coupling. However, the recent development of a partitioning method with a staggered solution approach as suggested by Park and Felippa[10], Paul[11] and Felippa and Geers[12] makes this approach very attractive. The major advantage of this method is that the coupled field problems can be tackled in a sequential manner. The analysis is carried out for each field and interaction effect is accounted for by updating the field variables of both the fields in the respective coupling terms. Though the method is iterative the number of variables in the fluid is one at each node for a linear fluid behaviour. For three-dimensional fluid–structure interaction studies this is quite beneficial. Another advantage of this approach is that it is modular in nature. Various fluid transient codes can be coupled to a structure dynamics code to study the interaction effects. Further, the modular adaptation makes this approach very attractive in a parallel processing environment.

The present paper demonstrates the capability to analyse three-dimensional fluid–structure interaction problems in an optimum manner by the method of partitioning. The structure response is obtained through the use of C^0 degenerate shell elements. This element, with associated through the thickness numerical integration, was introduced by Ahmad et al. [15] for linear static analysis. A number of deficiencies have been found in this element in the last decade. Studies with regard to locking behaviour and zero energy modes have helped to improve the performance of this element. Further, this element has not been used extensively to tackle problems of shell dynamics and coupled problems due to its cumbersome formulation requiring large computational time. Efficient two-dimensional degenerate shell elements based on explicit through thickness integration due to Belytschko[16] and Milford and Schnobrich[17] have recently been developed. The present paper demonstrates the capability of its effective implementation for coupled dynamic problems. The fluid transient behaviour is studied with three-dimensional brick elements. The presence variable is the only unknown at nodal points, to keep the number of degrees of freedom to a minimum in the fluid domain. The shell and fluid meshes are coupled in an optimum manner by assigning a separate equation numbering system for coupling terms to overcome the bandwidth problem described earlier. In the present work the nine-noded degenerate shell element has been used for shell dynamics, which gives the best combination of economy and accuracy as demonstrated by Pugh et al. [18] after comparing the performance of four-, eight-, nine-, 12- and 16-noded quadrilateral elements. The fluid transient behaviour is studied by an eight-noded trilinear brick element.

This element is sufficient to obtain dynamic loading on the shell surface in an accurate and economical way.

Another important aspect of transient analysis is the selection of an optimum integrator for second-order ordinary differential equations resulting from semidiscretization. There are two well known methods reported in the literature [11, 13, 19–24], implicit method and explicit method. Implicit methods are unconditionally stable and larger time steps can be used based on the order of accuracy required. However, the computational effort required is more in this case as the resulting simultaneous equations have to be solved at each time step. On the other hand, explicit methods are conditionally stable, thus time step size is limited by the minimum period of the mesh (or more simply by the period of the smallest element). However, in this method the CPU time and storage space required are small as it does not call for solution of a system of simultaneous equations. As described by Belytschko [13], transient problems are of two categories, wave propagation problems and inertial problems. For wave propagation problems the wave front has to be traced accurately, thus the number of modes which have to be integrated properly is very large. In the case of inertial problems, the response lies in a few lower modes and only these modes have to be integrated properly. Another important requirement of the integrator is that higher modes which are not important and which are associated with large errors must be filtered out. In the case of fluid–structure interaction problems, all the pressure modes in the fluid domain must be traced with accuracy if it is likely to affect the prominant structure modes. In the present work a mixed implicit–explicit scheme due to Hughes [19] has been used. Some aspects of mesh partitioning and selection of a proper integrator for fluid and shell domains are discussed.

The organization of the paper is as follows. In Sec. 2, we describe the formulation of the coupled shell fluid dynamics problem where shell dynamics and the fluid transient problem are discussed in detail. Section 3 describes the coupled equation solution strategy for the present problem and some guidelines are given to achieve efficient partitioning. In Sec. 4 a number of fluid–structure interaction problems are solved to demonstrate the capability of the present approach. The paper ends with conclusions for the effective use of the partitioning method for coupled problems.

2. COUPLED SHELL–FLUID DYNAMICS

In the present work coupled shell–fluid-dynamics problems have been analysed by solution of the shell dynamics equation and acoustic wave equation by finite element discretization. The resulting coupled second-order ordinary differential equations for two fields are numerically integrated by Newmark's

method. The fluid–structure interaction effect is studied by transferring the shell normal acceleration to the three-dimensional fluid domain and the fluid pressure to the shell surface at the shell–fluid interface for each time step in an iterative manner. Using this approach, single-field problems of shell dynamics or fluid transients (fluid with rigid boundaries) along with coupled shell–fluid dynamic problems can be analysed. The coupling at the shell–fluid interface is accounted for in a special manner by assigning a different equation numbering system to coupling matrices in order to achieve optimum computer storage space.

2.1. *Shell dynamics with two-dimensional degenerate shell elements*

Figure 1 shows a three-dimensional brick element with a quadratic displacement field description. This element can be degenerated to form a quadratic shell element. The shell geometry is either defined by top and bottom surface nodes of the shell element or by the middle surface nodes along with the thickness at each node point. Here a first-order shear deformation shell theory is used, in which it is assumed that the normal to the shell middle surface remains straight during deformation and strain energy corresponding to the shell normal stress is neglected.

In order to develop a two-dimensional degenerate shell element eight strains are defined at any point on the shell middle surface, viz. ϵ_{x0}, ϵ_{y0}, γ_{xy0}, κ_x, κ_y, κ_{xy}, γ_{xz0} and γ_{yz0}. Here an explicit integration in the thickness direction is used [16, 17] in the strain energy expression to obtain mid-surface stress resultants corresponding to these strains. This is called a two-dimensional model of a three-dimensional degenerate shell element. This method is different from the conventional approach [15, 20, 25] of considering five strains ϵ_x, ϵ_y, γ_{xy}, γ_{xz} and γ_{yz} at any point in the shell body and then either carrying out two-point Gaussian integration of element matrices (stiffness, mass or load) by taking linear variation of strain across the thickness or by a layered approach where a one-point Gaussian integration is applied for each layer. The present approach of a two-dimensional degenerate shell element with exact representation of inplane stress/strain across the thickness and explicit
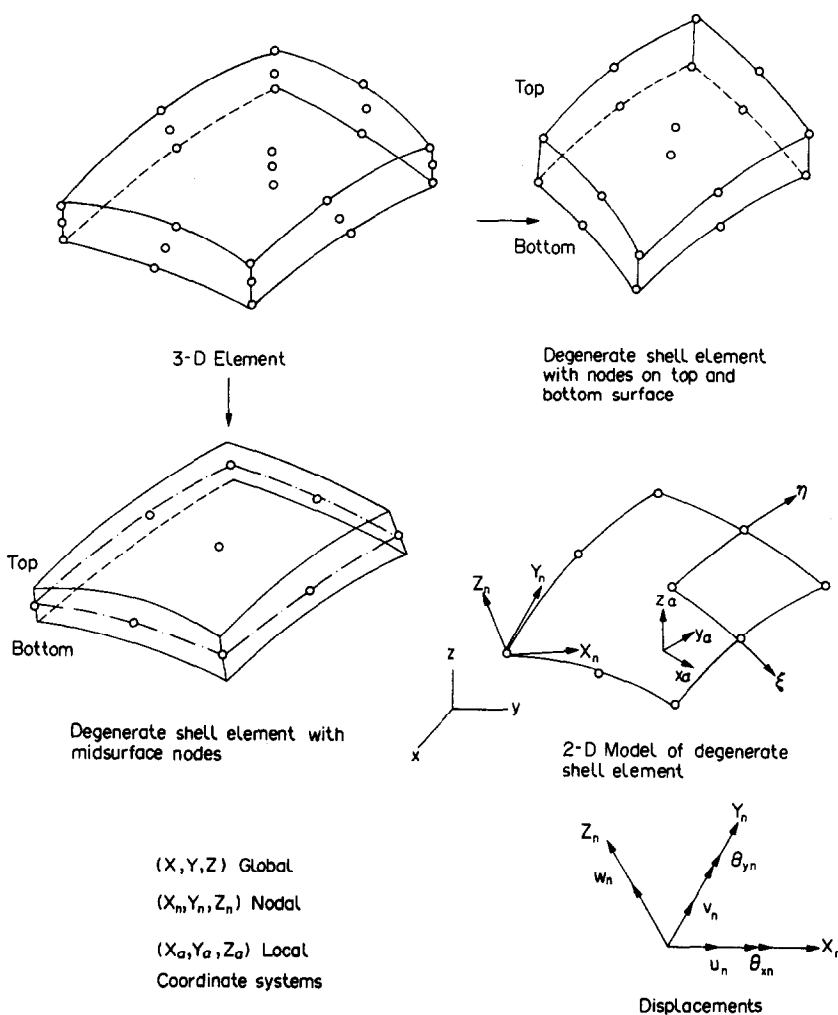
Fig. 1. Development of two-dimensional degenerate shell element.

integration results in computational ease and better accuracy than the conventional approach. This method is particularly suitable for coupled shell–fluid interaction problems, as shown in the latter part of the paper.

2.1.1. *Coordinate systems for two-dimensional degenerate shell element*. As shown in Fig. 1, three sets of coordinate systems, global (X, Y, Z), nodal (x_n, y_n, z_n) and local $(x_\alpha, y_\alpha, z_\alpha)$, are defined. The global coordinate defines the shell geometry. The nodal coordinate defines the nodal displacements and global stiffness, mass and load matrices. The local coordinate system is used for numerical integration of element matrices. Nodal and local coordinates are defined by a shell normal vector $V_\perp$ at a node n and any point α within the element by

$$V_\perp = V_\xi \times V_\eta, \tag{1}$$

where V_ξ and V_η are vectors along ξ and η natural coordinates of the shell element. Once the unit normal vector along $V_\perp$ (k_n at node n and k_α at point α within the element) is known, i_n or i_α for nodal or local coordinates is along V_ξ and j_n or j_α is thus finally defined by

$$j_{n,\alpha} = k_{n,\alpha} \times i_{n,\alpha}. \tag{2}$$

2.1.2. *Degenerate shell element matrices*. The two-dimensional degenerate shell element matrices are evaluated in the usual manner. Five generalized displacements at any point α in the element are defined as u_α, v_α, w_α, $\theta_{x\alpha}$ and $\theta_{y\alpha}$, consisting of three displacements and two rotations, respectively. The stresses and strains are defined in the local coordinate system, which is a very convenient way of representing the stress resultants. The displacements and strains in the element can be obtained by shape function N_s and strain displacement B matrices. At a node i in nodal coordinate system

$$\delta_{ni} = [u_{ni}, v_{ni}, w_{ni}, \theta_{xni}, \theta_{yni}]^T, \tag{3}$$

where δ_{ni} contains all the degrees of freedom at any node i.

Again

$$u^e = \sum_{i=1}^{node} N_{si} \delta_{ni}, \tag{4}$$

where u^e is the displacement field in the element. Strain at a point α in the element is defined in the local coordinate system as

$$\epsilon_\alpha = \sum_{i=1}^{node} B_i \delta_{\alpha i} \tag{5}$$

and

$$\delta_{\alpha i} = R_{\alpha i} \delta_{ni}, \tag{6}$$

where $R_{\alpha i}$ is the transformation matrix relating local displacement to nodal displacement and B_i is the strain–displacement matrix at any node i. Thus we have

$$\epsilon_\alpha = \sum_{i=1}^{node} B_i^* \delta_{ni}, \tag{7}$$

where

$$B_i^* = B_i R_{\alpha i}. \tag{8}$$

For the element the B^* matrix can be defined by augmenting contribution from all the nodes of the element as

$$B^* = [B_1^*, B_2^* \cdots B_i^* \cdots B_n^*]. \tag{9}$$

Thus, the element stiffness matrix is

$$(K_s^e)_{ij} = \int_{As} B_{im}^{*T} D_{mk} B_{kj}^* t \, dA_s, \tag{10}$$

where D is the elasticity matrix relating the mid-surface stress resultants and strains and t is the thickness of the shell. The element mass matrix with density ρ is

$$(M_s^e)_{ij} = \int_{As} \rho_s N_{si}^T N_{sj} t \, dA_s. \tag{11}$$

The consistent mass matrix can be converted into the lumped mass matrix as shown by Hinton *et al.* [26] and Surana [27]. For shells the lumping for rotational degrees of freedom terms is done by normalizing the diagonals by $m_i t_i^2/4$ [27], where m_i and t_i represent mass and thickness, respectively, at node i.

The above two-dimensional version of the degenerate shell element is very powerful for shell dynamics. A selective integration scheme [19, 25] is used for optimum behaviour of this element. The following semidiscrete equation of motion is formed which can be solved by any implicit, explicit or mixed time integration method.

$$M_s \ddot{u} + C_s \dot{u} + K_s u = f_s - M_s \ddot{u}_g, \tag{12}$$

where M_s, C_s and K_s are global mass, damping and stiffness matrices respectively, u is the global displacement and f_s is the external load. A superposed dot represents time derivative and $\ddot{u}_g$ is the specified ground acceleration. The structural damping matrix is constructed by

$$C_s = aM_s + bK_s. \tag{13}$$

The constants a and b may be choosen to control damping proportionately.

2.2. Fluid transients with three-dimensional fluid elements

In order to study the effect of shell–fluid interaction, three-dimensional modelling of the fluid domain is required. A number of finite element formulations are available, namely pressure formulation, displacement formulation, displacement potential and velocity potential formulation. These methods have been reviewed in the work of Paul [11]. The pressure formulation was chosen for the present work. The advantage of this method is that there is only one variable at each node (pressure). This results in significant computational economy in terms of computer time and storage space compared to other formulations, particularly for three-dimensional problems. Another advantage of this approach is that the pressure field obtained from the analysis of the fluid field can be directly transferred to the shell structure at the shell–fluid interface, unlike other methods where pressure has to be calculated from velocity or displacement or its potential. In the present work an eight-noded trilinear brick element has been developed to study the fluid transient behaviour. Since the shell response is of prime concern in most of the problems the trilinear fluid element is considered to be adequate for an optimum combination of economy and accuracy.

The governing acoustic wave equation in terms of dynamic pressure variable p for an inviscid, compressible fluid with small displacement is

$$\nabla^2 p = \frac{1}{c^2}\ddot{p} \text{ in fluid domain } \Omega_f, \tag{14}$$

where c is the acoustic speed. The three types of pressure gradients at the fluid boundary with outward normal n_f are as follows.

(i) Interaction boundary Γ_I with

$$p,n = -\rho_f \ddot{u}_n. \tag{15}$$

(ii) Free boundary Γ_F with

$$p,n = -\dot{p}/g. \tag{16}$$

(iii) Radiation boundary Γ_R with

$$p,n = -\dot{p}/c. \tag{17}$$

ρ_f, $\ddot{u}_n$ and g are the fluid density, shell normal acceleration at the shell–fluid interface and acceleration due to gravity, respectively. It may be noted that eqn (15) becomes homogeneous for a fluid interacting with a rigid boundary. Another type of boundary is for prescribed pressure p^s

$$p = p^s \text{ on } \Gamma_p. \tag{18}$$

The above boundaries define the fluid boundary Γ_f completely.

$$\Gamma_f = \Gamma_I + \Gamma_R + \Gamma_F + \Gamma_P. \tag{19}$$

The governing equation (14) along with boundary conditions (15)–(18) can be shown to result in an equation of the following form after semidiscretization.

$$\mathbf{M}_f\ddot{\mathbf{p}} + \mathbf{C}_f\dot{\mathbf{p}} + \mathbf{K}_f\mathbf{p} = \rho_f\mathbf{Q}_f(\ddot{\mathbf{u}} + \ddot{\mathbf{u}}_g) + \mathbf{f}_f, \tag{20}$$

where $\mathbf{M}_f$, $\mathbf{C}_f$ and $\mathbf{K}_f$ are the global fluid mass, damping and stiffness matrices, respectively. $\mathbf{Q}_f$ couples the fluid equations to structure and ground acceleration vectors $\ddot{\mathbf{u}}$ and $\ddot{\mathbf{u}}_g$, respectively, and $\mathbf{f}_f$ is the fluid force vector.

The above global matrices can be assembled from the fluid element matrices, which can be described as follows. Pressure in the element is given by the fluid element shape function $\mathbf{N}_f$ and nodal pressure $\mathbf{p}$ as

$$p = \mathbf{N}_f\mathbf{p}. \tag{21}$$

The fluid element mass matrix is obtained by impulsive and free surface sloshing terms as

$$(\mathbf{M}_f^e)_{ij} = 1/c^2 \int_{\Omega_f} N_{fi}^T N_{fj}\,d\Omega_f$$
$$+ 1/g \int_{\Gamma_F} N_{fi}^T N_{fj}\,d\Gamma_F. \tag{22}$$

The fluid element radiation damping matrix is considered for a nonreflecting boundary Γ_R as

$$(\mathbf{C}_f^e)_{ij} = 1/c \int_{\Gamma_R} N_{fi}^T N_{fj}\,d\Gamma_R. \tag{23}$$

Finally, the fluid element stiffness matrix is

$$(\mathbf{K}_f^e)_{ij} = \int_{\Omega_f} (N_{fi},x N_{fj},x + N_{fi},y N_{fj},y$$
$$+ N_{fi},z N_{fj},z)\,d\Omega_f. \tag{24}$$

The coupling matrix $\mathbf{Q}_f$ for the fluid domain is given by

$$(\mathbf{Q}_f)_{ij} = \int_{\Gamma_I} N_{fi}^T n_s N_{sj}\,d\Gamma_I, \tag{25}$$

where n_s gives the unit normal component at the shell surface on the shell–fluid interface.

2.3. Coupled shell–fluid systems

The semidiscrete shell dynamics equations (12) for a shell coupled with an acoustic medium of

the above description is modified with coupling term Q_s as

$$M_s\ddot{u} + C_s\dot{u} + K_su = f_s - M_s\ddot{u}_g + Q_sp. \qquad (26)$$

It may be easily recognised that the coupling matrices hold the relation $Q_s = -Q_f^T$. The system of equations (20) and (26) are coupled second-order ordinary differential equations which define the coupled shell–fluid system completely. These sets of coupled equations are solved on two different meshes of fluid and shell in a staggered fashion—a scheme proposed by Park and Felippa [10], Paul [11] and Felippa and Geers [12]. The advantage of the two-dimensional degenerate shell element presented in Sect. 2.1 may be noted here. The nodal coordinate system in the shell formulation gives the normal shell acceleration, which can be directly used with the coupling matrix Q_f in eqn (20). Similarly, the fluid pressure at the shell–fluid interface can be directly introduced with the coupling matrix Q_s of eqn (26). The pressure at midside nodes of shell element edges and at the element centre ($\xi = 0.0$ and $\eta = 0.0$) are linearly interpolated from the corner node values of a three-dimensional fluid element at the shell–fluid interface. A separate equation numbering system is evolved at the shell–fluid interface in the skyline solution procedure by keeping only active degrees of freedom (one at each node) at the interface. Finally, the coupling terms in the load vectors are transferred to the original equations of shell and fluid domains. This scheme requires minimum computer storage space for coupling matrices and is very powerful for three-dimensional shell–fluid interaction problems, particularly on small computers with inherent limitations on storage space.

3. TIME INTEGRATION OF COUPLED FIELD EQUATIONS

The set of coupled second-order ordinary differential equations (20) and (26) are solved by method of partitioning. The coupling terms make the set of equations unsymmetric, so the equations of each field should be solved in sequence. The interaction effect between the two fields is studied by transferring field variables from one field to another field at each time step in a staggered manner. This approach requires minimum storage space, as bandedness of equations is maintained. Another advantage of this approach is that the same time integrator can be applied to both the fields. In the present work Newmark's predictor–multi-corrector algorithm due to Hughes [19] has been used, which has been proven to be very powerful for such coupled problems [11]. This method recognises each element of either field as explicit or implicit. Thus a purely explicit or implicit integration method along with mixed explicit–implicit method can be used for one or both of the fields. The critical time steps for the fluid and shell elements are of

verying magnitude, thus this integration scheme allows significant flexibility in selecting an optimum integration scheme from a stability, accuracy and convergence point of view.

As a general guideline, in most of the practical cases the fluid field integrator may be fully explicit, since the critical time period for the fluid domain is normally orders of magnitude larger than the critical time period of the shell domain for the same mesh size. The shell equations could be treated by implicit method as the critical time period in this case is normally so low that an explicit integration method will require very large computational time, overshadowing the advantage of the lesser computational effort and time required at each time step. The explicit integration for the fluid field is particularly advantageous in the present case compared to the implicit integration. The latter will require large computer storage space. In addition, it results in the burden of solving a huge system of simultaneous equations, obtained from three-dimensional discretization, at each time step. The present formulation with quadratic displacement field description for the shell domain and linear pressure field description for the fluid domain is very powerful. Here the nodal spacing in the fluid domain is twice that of the shell domain, which allows the above type of explicit–implicit partitioning for fluid and shell meshes more conveniently. In the next paragraph we present the predictor–multi-corrector algorithm [11, 13, 19] for the semidiscrete coupled second-order equations (20) and (26) used in the present work.

The governing second-order equation at time step $n + 1$ is given by

$$M\ddot{u}_{n+1} + C\dot{u}_{n+1} + Ku_{n+1} = F_{n+1}. \qquad (27)$$

Here the subscript has been dropped as it may be used for any field. The force term augments applied force, specified boundary conditions and interaction terms from the other field. In the predictor phase the field variables are expressed as

$$u_{n+1}^i = \tilde{u}_{n+1} \qquad (28)$$

$$\dot{u}_{n+1}^i = \tilde{\dot{u}}_{n+1} \qquad (29)$$

$$\ddot{u}_{n+1}^i = 0, \qquad (30)$$

where i is the iteration count and

$$\tilde{\dot{u}}_{n+1} = \dot{u}_n + \Delta t(1 - \gamma)\ddot{u}_n \qquad (31)$$

$$\tilde{u}_{n+1} = u_n + \Delta t\,\dot{u}_n + 1/2\,\Delta t^2(1 - 2\beta)\ddot{u}_n. \qquad (32)$$

Here γ and β are Newmark's parameters and Δt is the time step.

In the solution phase the following equation is formed and solved.

$$K^* \Delta u^i = f_{n+1}^{*i}, \qquad (33)$$

where

$$K^* = M/\beta \, \Delta t^2 + \gamma C/\beta \, \Delta t + K \qquad (34)$$

and

$$f_{n+1}^{*i} = F_{n+1}^i - M\ddot{u}_{n+1}^i - C\dot{u}_{n+1}^i - Ku_{n+1}^i. \qquad (35)$$

Once the increment in the field variable is obtained, field variables are updated as follows:

$$u_{n+1}^{i+1} = u_{n+1}^i + \Delta u^i \qquad (36)$$

$$\ddot{u}_{n+1}^{i+1} = (u_{n+1}^{i+1} - \tilde{u}_{n+1})/\beta \, \Delta t^2 \qquad (37)$$

$$\dot{u}_{n+1}^{i+1} = \dot{u}_{n+1}^i + \gamma \, \Delta t \, \ddot{u}_{n+1}^{i+1}. \qquad (38)$$

Finally, a convergence check is made on the norm of the increment in the field variable compared to the norm of the total field variable as follows.

Is $\|\Delta u^i\|/\|u^{i+1}\| \leqslant e$ (the specified tolerance)?   (39)

If NO, $i \to i + 1$, and go to eqn (33) for next iteration.

If YES, $n \to n + 1$, and go to eqn (27) for next time step.

Element-wise mesh partitioning is done by recognizing elements as explicit or as implicit,

$$M = M^I + M^E \qquad (40)$$

$$C = C^I + C^E \qquad (41)$$

$$K = K^I + K^E \qquad (42)$$

$$F = F^I + F^E, \qquad (43)$$

and modifying the governing equation (27) as

$$M^I\ddot{u}_{n+1} + M^E\ddot{u}_{n+1} + C^I\dot{u}_{n+1} + K^I u_{n+1}$$
$$= F_{n+1}^I + F_{n+1}^E. \qquad (44)$$

The stability criterion of Newmark's integrator for a single field with a single pass is well established [13, 19, 21]. $\gamma \geqslant 1/2$ and $\beta = (\gamma + 1/2)^2/4$ leads to unconditional stability. In the case of coupled problems the stability criterion is a function of mesh integrator, predictor formula and computational path [10–12]. Analytical evaluation of the critical time step is difficult in the present case as the order of the characteristic polynomial for stability analysis is large. However, in the present formulation the interaction term appears as a force term, which may be regarded as similar to the pseudo force term of a nonlinear dynamics problem. Therefore, a small reduction in the time step (approx. 10–20% of the critical time step) is desirable, as suggested by Belytschko [3] for nonlinear problems, in order to achieve rapid convergence.

4. NUMERICAL EXAMPLES

A computer code FLUSHEL [28] has been developed by the present authors to study the performance of the present formulation. This code can be used to solve single-field problems of shell dynamics or fluid transients along with the coupled shell–fluid interaction problems. A number of problems have been solved with Newmark's parameters $\beta = 0.25$ and $\gamma = 0.5$ and a tolerence $e = 1.0\,E - 05$ for convergence criteria by explicit and implicit methods. The results reported here have been obtained on a NORSK DATA machine ND 560 in double precision. The problems presented here have been taken from the paper of Akkas et al. [5], where the results were reported for a continuum mechanics approach.

4.1. Pressure wave propagation problem

Figure 2a shows the problem of pressure wave propagation in a rigid pipe. A 20-in.-long pipe with a cross-section of 4×4 in. containing fluid has been analysed for a pressure pulse of 1 psi applied at one end. The other end of the pipe is closed with a steel cap. The fluid domain has been modelled with 20 eight-noded brick elements. Solution has been obtained for the fluid domain with a homogeneous boundary, i.e. the fluid boundary is assumed to be surrounded by a rigid pipe. A time step of 0.028 msec has been used, which is the critical time step for this
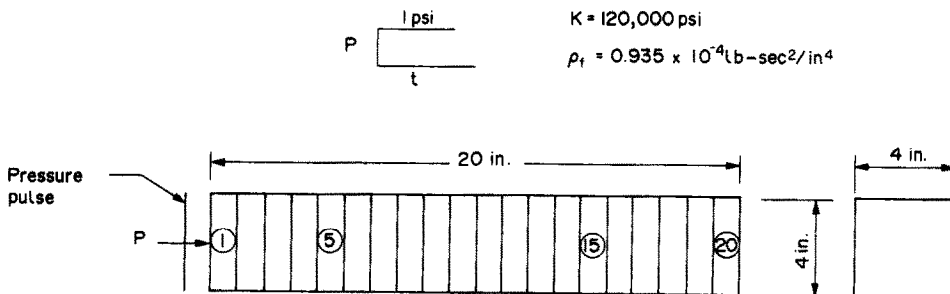
Fig. 2a. Pressure wave propagation in a pipe.
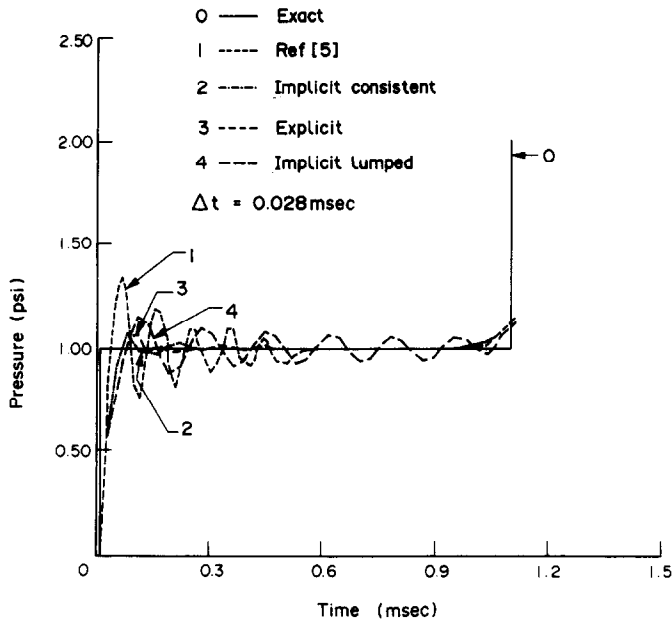
Fig. 2b. Pressure history in element 1.

mesh obtained from eigenvalue analysis. This is of same order as h/c, where h is the mesh size along the axis of the fluid domain. Results are shown in Figs 2b–2e at the centre of elements 1, 5, 15 and 20 for the case of implicit integration with a consistent mass matrix of fluid, explicit integration with a lumped mass and implicit integration with a lumped mass. In the same figures the exact results and results of [5] are also shown. The numerical results of Akkas et al. [5] and the present results show dispersion or oscillatory behaviour at the shock front due to discontinuity, and spatial and temporal discretization errors as discussed by

Schreyer [29]. It may be inferred from the nature of the results that the matched method of time integration, i.e. explicit method with lumped mass and implicit method with consistent mass, represents the scock wave more accurately. This has been discussed in detail by Hughes [19], where the theoretical argument given is that spatial and temporal discretization errors tend to concel each other in matched method. It is realized from the present example that the explicit method with a lumped mass matrix can be used effectively to trace the shock wave in an economic way for three-dimensional problems.
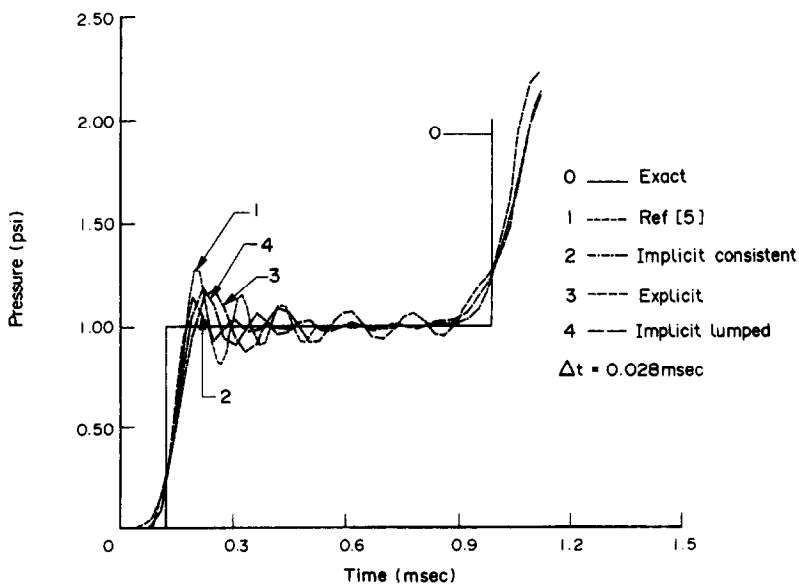
Fig. 2c. Pressure history in element 5.
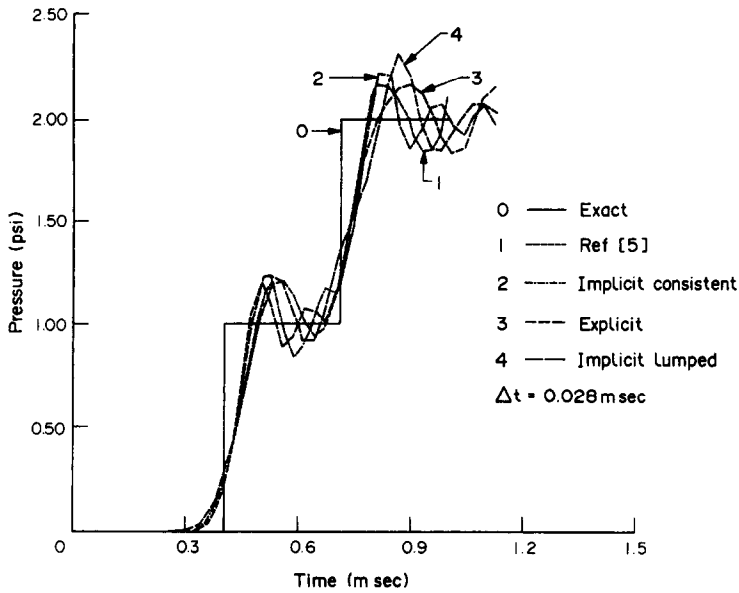
Fig. 2d. Pressure history in element 15.

4.2. *Plate–fluid interaction problem*

In Fig. 3a the problem of a fluid reservoir (150 cm × 100 cm × 50 cm) supported by a steel plate (5 cm × 100 cm × 50 cm) at one end is shown. At the other end of the reservoir a pressure pulse of 100 kg/cm² is applied. The pressure history is traced at point A ($x = 142.5$ cm, $y = 75$ cm) in the fluid domain. The analysis has been carried with a 15 × 10 × 1 mesh of the fluid domain with eight-noded brick elements. The steel plate is modelled with 10 nine-noded shell elements. The critical time steps for fluid and shell meshes are 0.035 and 0.0039 msec, respectively. Here an explicit–implicit (E–I) partitioning for fluid and shell meshes can be used, since the

time step for the shell is more critical. Transient analysis has been carried with a time step of 0.032 msec. Figure 3b shows the results, and the results due to Akkas *et al.* [5] are also shown for the rigid plate case and the flexible plate case. Again the pressure history shows oscillation near the shock front for the rigid plate case compared to the exact solution. However, it is less than that reported in [5] due to proper selection of the integrating scheme and mass matrix. In the case where the solution is obtained by taking into account the flexibility of the steel plate, the pressure history is lower than that reported in [5]. The results of [5] are based on bilinear two-dimensional plane strain elements, where only one element has been taken across the thickness of
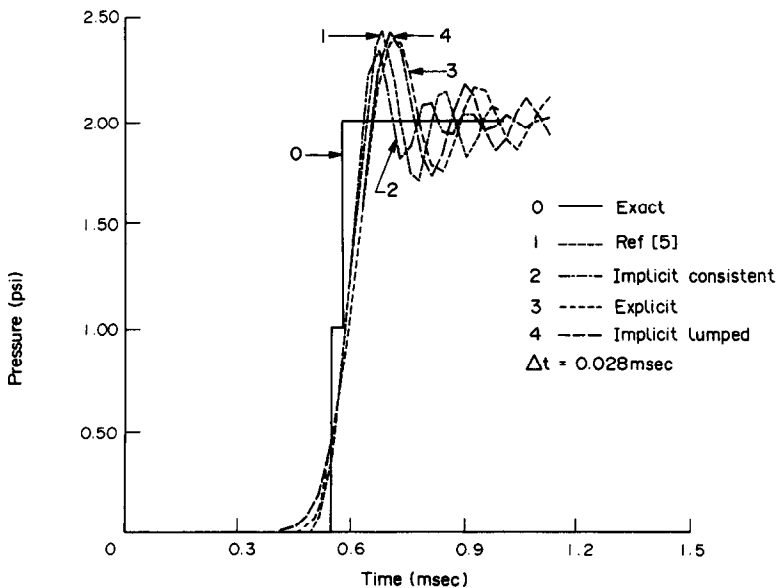
Fig. 2e. Pressure history in element 20.
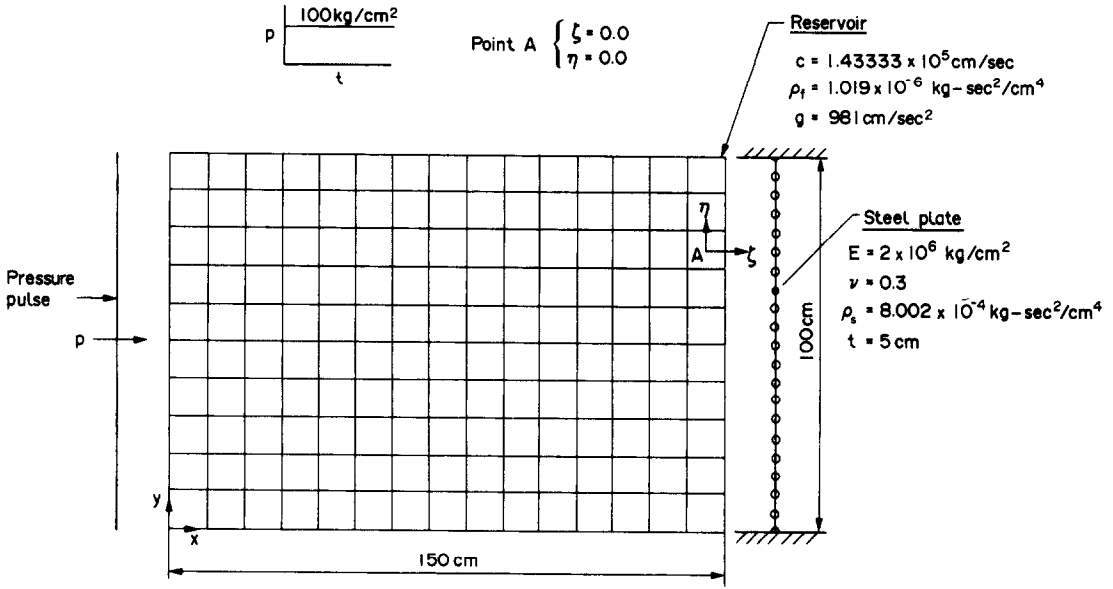
Fig. 3a. Plate–fluid interaction problem.

the plate. This element is known to be very stiff in bending, so the reported pressure is high. In order to check this, the results have been compared with the two-dimensional results of Singh et al. [30] with code FLUSOL, which is a two-dimensional code for fluid–structure interaction. In two-dimensional anlaysis the fluid has been modelled with 5×5 nine-noded plane fluid elements and the plate has been modelled with a 5×1 mesh of nine-noded plane stress elements. As shown in Fig. 3b, the two-dimensional results match well with the present three-dimensional fluid and shell element results.

4.3. Reservoir with base motion

Problems of water reservoirs and fluid tanks subjected to base excitation are one of the important areas where considerable attention has been

created [4, 31–36]. We now present the problem of a water reservoir of 300 ft × 300 ft size which is subjected to a constant acceleration of 1.0 g at the base. If the fluid boundary is assumed to be surrounded by a rigid wall, comparison can be made with the exact pressure history available due to Chopra et al. [31] and two-dimensional finite element results due to Akkas et al. [5]. Figure 4 shows the impulsive pressure history at $x = 30$ ft and $y = 30$ ft from the base for a three-dimensional fluid model with $6 \times 5 \times 1$ mesh by implicit and explicit integration methods, with a time step of 2.5 msec. In the same figure, the two-dimensional finite element results of Akkas et al. [5] are also shown by direct integration (DI) and mode superposition (M-S) methods. It may be noted here that the present results trace the impulsive pressure response more
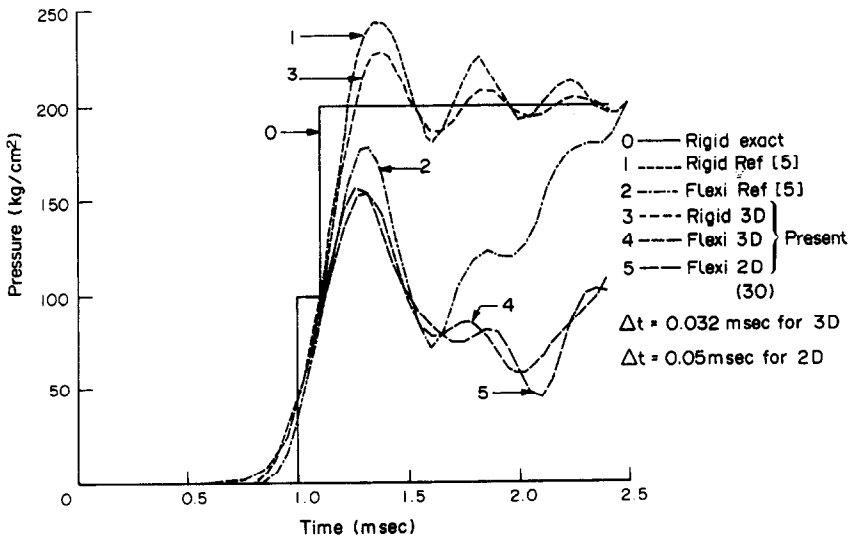
Fig. 3b. Plate–fluid interaction.
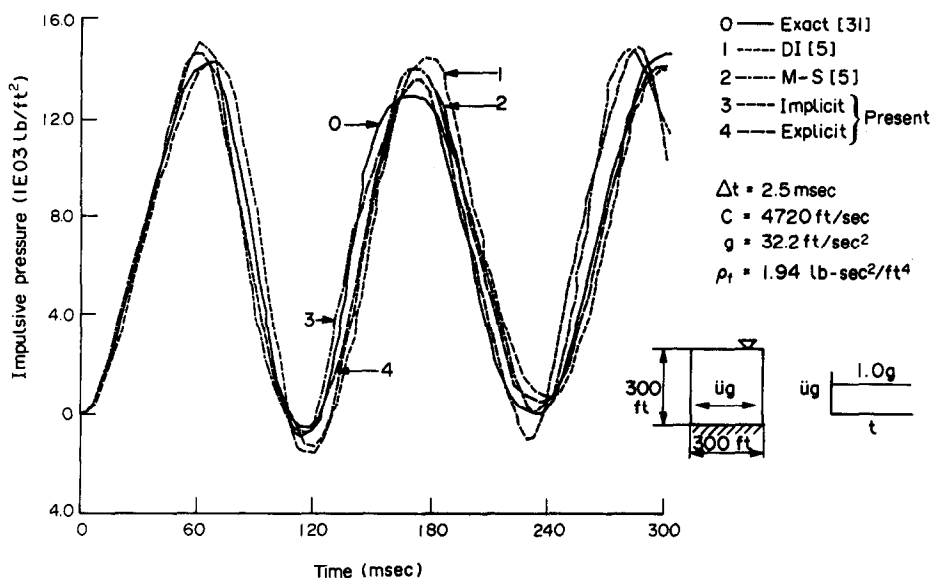
Fig. 4. Reservoir under base motion (three-dimensional result).

accurately than that given in [5]. The phase shift and amplitude change are a minimum for the present case. This is due to the fact that pressure is obtained directly in the present case, while in the continuum mechanics approach the pressure is obtained from the gradient of the displacement field. Some spurious modes are also present in these results due to circulation and presence of pseudo frequency, which is typical of continuum mechanics-based fluid elements, unless these are suppressed numerically.

4.4. Exterior shell–fluid interaction problem

One of the classical problems of shell–fluid interaction is that of a spherical shell submerged in an infinite acoustic medium. A spherical shell with inside radius of 75 in. and thickness of 1 in. has been taken for analysis. The shell is subjected to an impulsive internal pressure of 1.0186 psi and the pressure wave is traced at distances of 0.5, 9.5, 19.5 and 29.5 in. from the shell outer surface. Due to symmetry 2° sectors in circumferential·and longitudinal directions have been taken on the shell surface, which is modelled with a 2 × 2 element mesh. The surrounding fluid domain has been modelled with a 2 × 2 × 15 mesh of brick elements in the present case. The fluid mesh is taken up to a radial distance of 29.5 in. from the shell outer surface. A radiation boundary condition is applied at this end. The critical time steps for the fluid and shell meshes
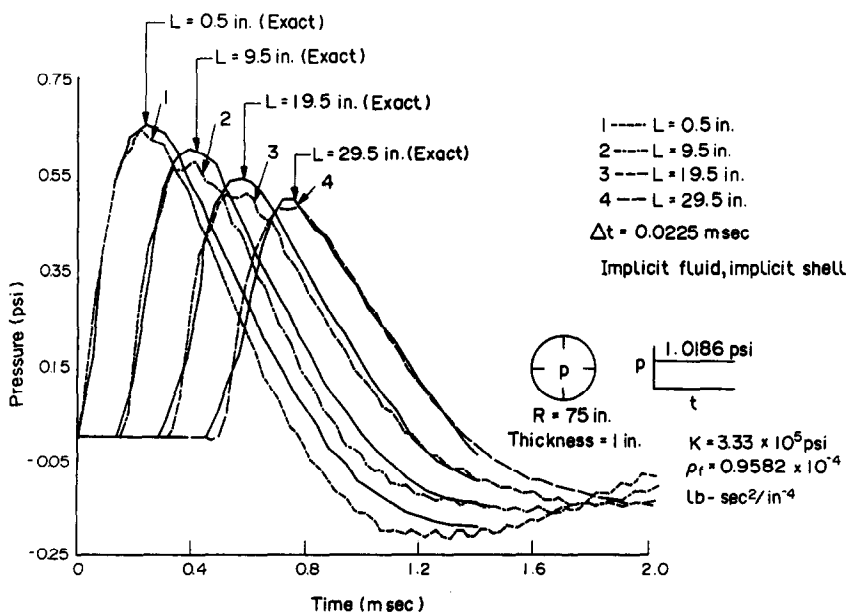
Fig. 5a. Pressure wave propagation from submerged sphere.
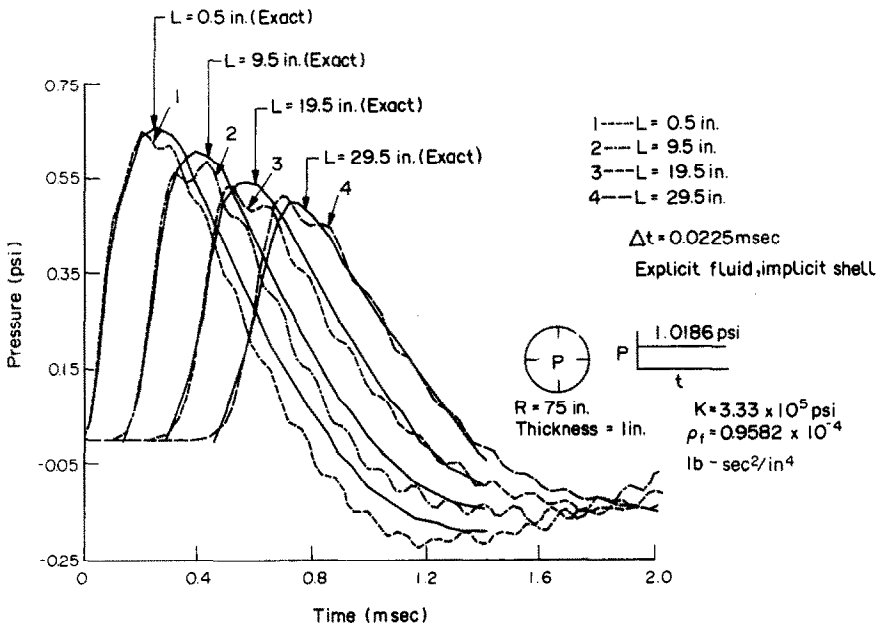
Fig. 5b. Pressure wave propagation from submerged sphere.

are 0.0233 and 0.00286 msec, respectively. Figure 5a shows the pressure wave propagation obtained by implicit–implicit (I–I) partitioning for fluid and shell meshes, respectively, with a time step of 0.0225 msec. Figure 5b shows the results with explicit–implicit (E–I) partitioning with same time step. In this case the fluid radiation damping matrix C_f is lumped in the same manner as M_f by a special lumping technique [26]. The radial deflection of the shell is shown in Fig. 5c and both types of partitionings give responses which overlap each other. The present results in all these cases match very well with the exact results [5].

4.5. Interior shell–fluid interaction problem

Another shell–fluid interaction problem of interest is that of a spherical shell containing fluid inside it. This problem has been solved by Akkas et al. [5] and Shugar and Katona [37]. The shell is subjected to an impact pressure of 100 kg/cm² applied at the shell top pole, as shown in Fig. 6. A sector of 30° in the circumferential direction and 180° in the longitudinal direction of the shell is modelled with proper symmetry conditions. The fluid mesh is made consistent with the outer shell cover. The analysis has been carried out for E–I and I–I partitionings of fluid and shell meshes for time steps of $1.25 \, E - 03$ msec and
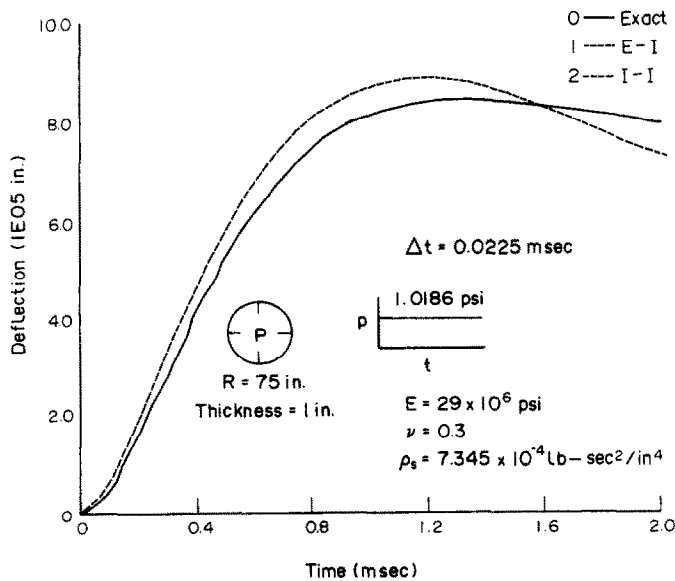
Fig. 5c. Radial deflection of submerged sphere.
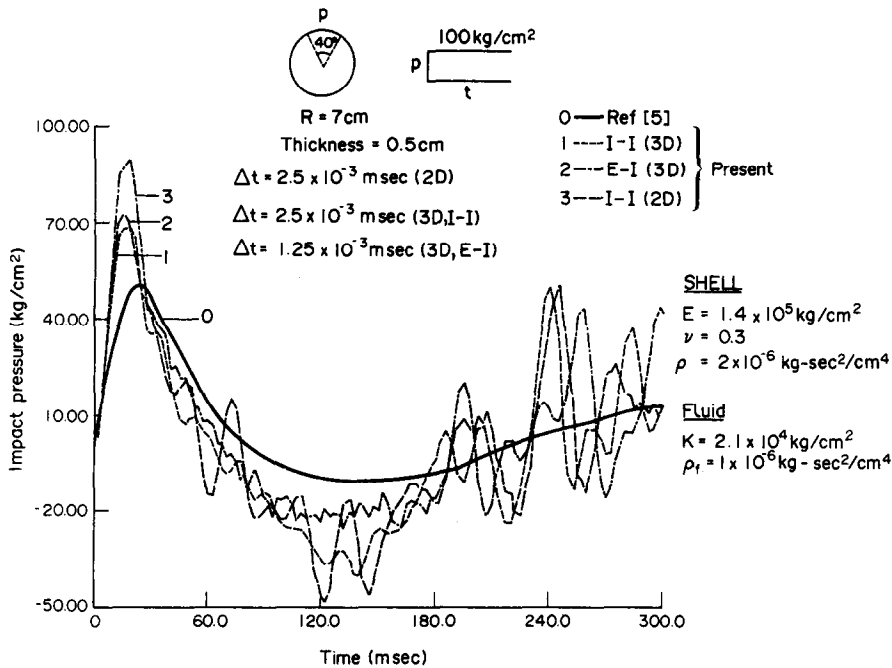
Fig. 6. Interior shell-fluid interaction.

2.5 E — 03 msec, respectively. The top pole pressure (at a radius of 6.5 cm and an angle of 5° from the vertical axis) in the fluid is compared with the results of [5] and [37]. The present results with the shell element show a higher peak pressure. Moreover, in the latter portion of the curve (approx. 0.2 msec) pressure again rises. This behaviour is not shown in the results of [5] or [37]. The second pressure peak is due to the superposition of the pressure wave reflected from the lower pole after 0.2 msec, which is the time required for the wave to reach the top pole after reflection from the lower pole. In order to check this again comparison has been made with results due to Singh et al. [30], where the analysis is carried out with two-dimensional axisymmetric elements available in code FLUSOL. The two-dimensional result with I–I partitioning with a time step of 2.5 E — 03 msec is also shown in Fig. 6. This result also shows the effect of the reflected wave after 0.2 msec.

5. CONCLUSIONS

Transient analysis of three-dimensional fluid–structure interaction problems has been demonstrated through an effective partitioning scheme. The present approach is economical in terms of the storage space and CPU time required for such problems. The economical implementation has been achieved through a displacement-based two-dimensional degenerate C^0 shell element and a three-dimensional fluid element with only pressure variables as unknowns at nodal points. An explicit integration scheme for the fluid domain (which is normally of large size) and an implicit scheme for the shell structure makes this approach very attractive. By

assigning separate equation numbering to the coupling matrices and using a nodal coordinate system for the shell structure the storage requirement for the coupling matrices reduces to a minimum. A number of case studies presented in the present paper indicate that this formulation has potential for nonlinear fluid–structure interaction problems as an extension to the present approach.

REFERENCES

1. K. J. Bathe and W. F. Hahn, On transient analysis of fluid–structure systems. *Comput. Struct.* **10**, 383–391 (1979).
2. W. K. Liu and H. G. Chang, A method of computation for fluid structure interaction. *Comput. Struct.* **20**, 311–320 (1985).
3. T. Belytschko, Fluid–structure interaction. *Comput. Struct.* **12**, 459–469 (1980).
4. W. K. Liu, Development of finite element procedures for fluid structures interaction. Ph.D. thesis, EERL 80–86, Californian Institute of Technology, University of California at Berkeley, CA (1981).
5. N. Akkas, H. U. Akay and C. Yilmaz, Applicability of general purpose finite element programes in solid–fluid interaction problems. *Comput. Struct.* **10**, 773–783 (1979).
6. E. L. Wilson and M. Khalvati, Finite elements for the dynamic analysis of fluid–solid systems. *Int. J. Numer. Meth. Engng* **19**, 1657–1668 (1983).
7. D. Shantaram, D. R. J. Owen and O. C. Zienkiewicz, Dynamic transient behaviour of two or three dimensional structures, including plasticity, large deformation effects and fluid interaction. *Earthquake Engng. struct. Dynam.* **4**, 561–576 (1976).
8. S. S. Deshpande, R. M. Belkune and C. K. Ramesh., Dynamic analysis of coupled fluid–structure interaction problems. In *Numerical Methods for Coupled Problems* (Edited by E. Hinton, P. Bettes and R. W. Lewis), pp. 367–378. Pineridge Press, Swansea, U. K. (1981).

9. M. K. Au-Yang and J. E. Galford, Fluid–structure interaction—a survey with emphasis on its application to nuclear steam system design. *Nucl. Engng Des.* **70,** 387–399 (1982).

10. K. C. Park and C. A. Felippa, Partitioned analysis of coupled systems. In *Computational Methods for Transient Analysis* (Edited by T. Belytschko and T. J. R. Hughes), Ch. 4. North Holland, Amsterdam (1983).

11. D. K. Paul, Single and coupled multifield problems. Ph.D. thesis c/ph/64/82, University College of Swansea, University of Wales, U.K. (1982).

12. C. A. Felippa and T. L. Geers, Partitioned analysis for coupled mechanical systems. *Engng Comput.* **5,** 123–133 (1988).

13. T. Belytschko and T. J. R. Hughes (Eds), *Computational Methods for Transient Analysis.* North Holland, Amsterdam (1983).

14. T. L. Geers and C. Ruzicka, Finite element/boundary element analysis of multiple structures excited by transient acoustic waves. In *Numerical Methods for Transient and Coupled Problems* (Edited by R. W. Lewis, P. Bettes and E. Hinton), pp. 150–162. Pineridge Press, Swansea, U.K. (1984).

15. S. Ahmad, B. M. Irons and O. C. Zienkiewicz, Analysis of thick and thin shell structures by curved elements. *Int. J. Numer. Meth. Engng* **2,** 419–451 (1970).

16. T. Belytschko, Stress projection for membrane and shear locking in shell finite element. *Comput. Meth. appl. Mech. Engng* **51,** 221–258 (1985).

17. R. V. Milford and W. C. Schnobrich, Degenerated isoparametric finite elements using explicit integration. *Int. J. Numer. Meth. Engng* **23,** 133–154 (1986).

18. E. D. L. Pugh, E. Hinton and O. C. Zienkiewicz, A study of quadrilateral plate bending elements with reduced integration. *Int. J. Numer. Meth. Engng* **12,** 1059–1079 (1978).

19. T. J. R. Hughes, *The Finite Element Method.* Prentice–Hall, Englewood Cliffs, NJ (1987).

20. D. R. J. Owen and E. Hinton, *Finite Elements in Plasticity: Theory and Practice.* Pineridge Press, Swansea, U.K. (1980).

21. O. C. Zienkiewicz, *The Finite Element Method,* 3rd Edn. McGraw–Hill, London (1976).

22. T. Belytschko, A survey of numerical methods and computer programs for dynamic structural analysis. *Nucl. Engng Des.* **37,** 23–24 (1976).

23. T. Belytschko and R. Mullen, Stability and explicit–implicit mesh partitions in time integration. *Int. J. Numer. Meth. Engng* **12,** 1575–1586 (1978).

24. T. Belytschko, H. J. Yen and R. Mullen, Mixed methods for time integration. *Comput. Meth. appl. Mech. Engng* **17/18,** 259–275 (1979).

25. E. Hinton and D. R. J. Owen, *Finite Element Software for Plates and Shells.* Pineridge Press, Swansea, U. K. (1984).

26. E. Hinton, T. Rock. and O. C. Zienkiewicz, A note on mass lumping and realted processes in the finite element method. *Earthquake Engng struct. Dynam.* **4,** 245–249 (1976).

27. K. S. Surana, Lumped mass matrices with non-zero inertia for general shell and axi-symmetric shell elements. *Int. J. Numer. Meth. Engng* **12,** 1635–1650 (1978).

28. R. K. Singh, T. Kant and A. Kakodkar, Studies of shell fluid interaction problems. In *Engineering Software* (Edited by C. V. Ramakrishnan, A. Varadarajan and C. S. Desai) (Proc., International Conference, ICENSOFT-89, 4–7 December 1989, New Delhi), pp. 865–872. Narosa, New Delhi (1989).

29. H. L. Schreyer, Dispersion of semidiscretized and fully discretized systems. In *Computational Methods for Transient Analysis* (Edited by T. Belytschko and T. J. R. Hughes), Ch. 6. North-Holland, Amsterdam (1983).

30. R. K. Singh, A. Kakodkar and T. Kant, Some studies on fluid structure interaction problems. Report No. BARC-1424, BARC, Trombay, Bombay (1988).

31. A. K., Chorpa, E. L. Wilson and L. Farhoomand, Earthquake analysis of reservoir dam systems. Proc. 4th World Conference on Earthquake Engineering, Santiago, Chile (1969).

32. P. Chakrabarti and A. K. Chopra, Earthquake response of gravity dams including reservoir interaction effects. EERC 72-6, University of California, Berkeley, CA (1972).

33. N. M. Newmark and E. Resenblueth, *Fundamentals of Earthquake Engineering.* Prentice–Hall, Englewood Cliffs, NJ (1971).

34. J. R. Roberts, E. R. Basurto and P. Y. Chen, Slosh design handbook 1. NAS 8-11111, Northrop Space Laboratories, Huntsville, AL (1966).

35. D. D. Kana, Status and research needs for prediction of seismic response in liquid containers. *Nucl. Engng Des.* **69,** 205–221 (1982).

36. D. C. Ma, J. Gvildys and Y. W. Chang, Seismic behaviour of liquid-filled shells. *Nucl. Engng Des.* **70,** 437–455 (1982).

37. T. A. Shugar and M. G. Katona, Development of finite element head injury model. *J. Engng Mech. Div, ASCE* **101,** 223–239 (1975).